The Astrophysical Journal, 701:635–641, 2009 August 10 doi:10.1088/0004-637X/701/1/635

ON THE PROSPECT OF CONSTRAINING BLACK HOLE SPIN THROUGH X-RAY SPECTROSCOPY OF HOTSPOTS

Kendrah D. Murphy[1,2], Tahir Yaqoob[2,3], Vladimir Karas[4], and Michal Dovčiak[4]

[1] MIT Kavli Institute for Astrophysics and Space Research, 77 Massachusetts Avenue, NE 80, Cambridge, MA 02139, USA

[2] Department of Physics and Astronomy, Johns Hopkins University, Baltimore, MD 21218, USA

[3] Astrophysics Science Division, NASA/Goddard Space Flight Center, Greenbelt, MD 20771, USA

[4] Astronomical Institute, Academy of Sciences, Boční II, CZ-141 31 Prague, Czech Republic

Received 2009 March 31; accepted 2009 June 17; published 2009 July 24

ABSTRACT

Future X-ray instrumentation is expected to allow us to significantly improve the constraints derived from the Fe K lines in active galactic nuclei, such as the black hole angular momentum (spin) and the inclination angle of the putative accretion disk. We consider the possibility that measurements of the persistent, time-averaged Fe K line emission from the disk could be supplemented by the observation of a localized flare, or "hotspot," orbiting close to the black hole. Although observationally challenging, such measurements would recover some of the information loss that is inherent to the radially integrated line profiles. We present calculations for this scenario to assess the extent to which, in principle, black hole spin may be measured. We quantify the feasibility of this approach using realistic assumptions about likely measurement uncertainties.

Key words: black hole physics – galaxies: active – line: profiles – X-rays: galaxies

1. INTRODUCTION

Black holes are often described as having "no hair" as there are only three characteristic quantities that define them: mass, charge,[5] and angular momentum. Evaluating the black hole metric ("Kerr" metric, or when charge is nonzero, "Kerr–Newman" metric) amounts to accurate measurement of these quantities. Ultimately these parameters will be critical for testing general relativity. The masses of black holes are measurable and there are continual advances in mass-measurement methods (e.g., Peterson & Benz 2008, and references therein). As yet, however, a method for measuring black hole charge has not been discovered. The electric charge is usually assumed to be zero since astronomical black holes are embedded in plasma, so the process of selective charge accretion gradually diminishes the charge to insignificant levels. It is therefore essential to determine the angular momentum (spin) of a black hole in order to constrain its metric. In addition, the spin of the supermassive black hole found in an active galactic nucleus (AGN) is an important diagnostic of the system. For example, black hole spin is thought to power relativistic jets seen in some AGN sources (see Blandford & Znajek 1977). Furthermore, the growth history of supermassive black holes may involve spin evolution, ultimately affecting the present distribution of spins (e.g., King et al. 2008).

Accretion from a disk is thought to change the spin of a black hole until an equilibrium value is established. The spin can be expressed in the dimensionless geometrical units a/M (where M is the mass of the black hole), which has an absolute value between 0 (nonspinning, Schwarzschild black hole) and 1 (extreme Kerr black hole). It is suggested that the upper limit on spin due to accretion is $a/M \sim 0.9982$ (Thorne 1974), although this value has been challenged (e.g., Gammie et al. 2004; Beckwith et al. 2008). The influence of a rotating gravitational field on light is specific to general relativity. It is not reproduced in Newtonian theory (e.g., Islam 1985). The spin of a black hole determines the horizon radius ($R_{\rm H}$) and the radius of the marginally stable orbit ($R_{\rm MS}$), otherwise known as the innermost stable circular orbit (ISCO), two quantities that are predicted by general relativity. Figure 1 shows the dependence of $R_{\rm H}$ and $R_{\rm MS}$ (as functions of gravitational radius, $R_{\rm G} \equiv GM/c^2$; see e.g., Misner et al. 1973) on spin. The ISCO of a nonspinning black hole is located at $6R_{\rm G}$ from the center, but this radius shrinks to $1.227\,R_{\rm G}$ ($1.0\,R_{\rm G}$) for a black hole with $a/M = 0.9982$ (1.0).

Since we are unable to image the vicinity of the supermassive black hole in AGNs, the spectrum of the X-ray emission, which originates from the innermost regions of the system, is one of the best probes that we currently have of the strong-gravity regime of these systems. The Fe K emission line in the X-ray spectrum is also often used as a tool to probe the physical parameters of an AGN system. Narrow Fe K lines that are not relativistically shifted in energy, which are ubiquitous in AGN observations (see Yaqoob & Padmanabhan 2004), are most likely reprocessed emission from circumnuclear matter far from the central black hole and/or from the outer regions of the accretion disk. On the other hand, broad Fe K lines, which are detected less often, are most likely the product of emission that originates in the inner accretion disk (e.g., Nandra et al. 2007). This emission, which is subject to gravitational and relativistic Doppler shifting in energy, is therefore believed to uncover important information on the innermost regions of AGNs, including the spin of the black hole (e.g., see Brenneman & Reynolds 2006; Miller 2007, and references therein). Similar techniques have been applied to stellar-mass black holes in X-ray binary systems (e.g., Miller et al. 2008; Reis et al. 2009; Miller et al. 2009, & references therein). In addition to the relativistic Fe K emission-line, X-ray binaries (and in principle AGN as well) offer the possibility of constraining black hole spin from spectral-fitting of the accretion-disk continuum, which is influenced by relativistic effects in the strong gravity regime (e.g., see Shafee et al. 2006; McClintock et al. 2006; Miller et al. 2009, & references therein). It has also been suggested that black hole spin measurements in Galactic X-ray binary systems may be possible through timing measurements of the high-frequency quasi-periodic oscillations (QPOs; e.g., McClintock & Remillard 2006).

[5] This may include magnetic charge in addition to electric charge.

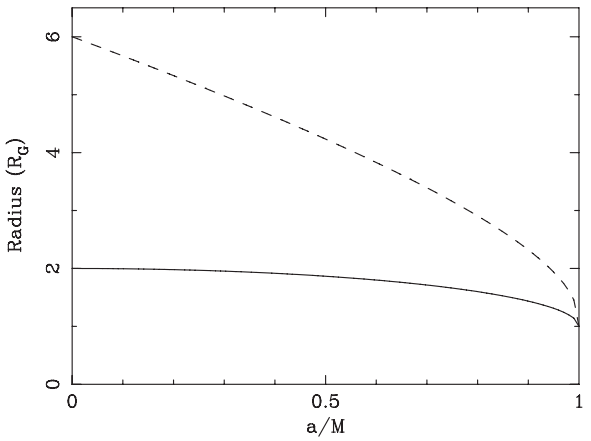

Figure 1. Distance (in gravitational radii) from the black hole to the horizon radius (R_H; solid) and to the marginally stable orbit (R_{MS}; dashed), vs. spin. See Misner et al. (1973).

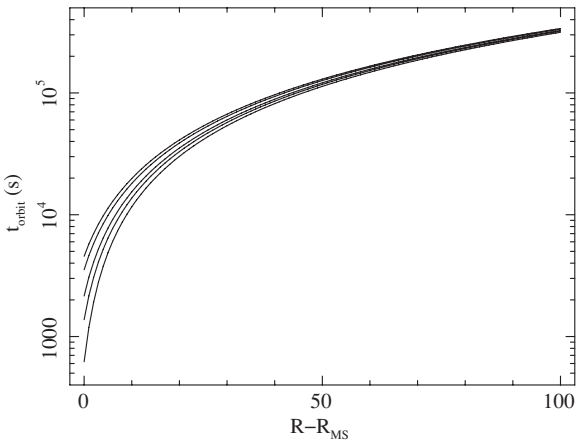

Figure 2. Orbital time vs. distance from the innermost stable circular orbit, in units of gravitational radii, for a black hole with a mass of $10^7\ M_\odot$. The orbital time can simply be scaled linearly for other masses. Curves are shown (top to bottom) for $a/M = 0,\ 0.3,\ 0.7,\ 0.9$, and 1.

In the present paper we describe a method to constrain black hole spin that involves measurements of Fe K lines resulting from localized, accretion-disk flares, or "hotspots" that orbit the black hole. The method relies on the measurement of the energies of narrow spectral features, and not line intensities. Some of the physical information that is lost in the radially integrated Fe K emission-line profiles is recovered, since the spatial scale that is probed by the hotspots is much smaller. In Section 2 we give a detailed description of how Fe K line hotspots may be used to constrain black hole spin and investigate the impact of likely observational uncertainties on the proposed method. The results of the investigation of the technique are described in Section 3. Our conclusions are summarized in Section 4.

2. MEASURING BLACK HOLE SPIN FROM LOCALIZED HOTSPOTS

It is theorized that X-ray flares can result from magnetic reconnection events that illuminate localized portions of the accretion disk, where the emission is reprocessed (e.g., Galeev et al. 1979; Czerny et al. 2004, and references therein). These compact "hotspots" temporarily enhance the continuum and Fe K line emission from the localized region of the accretion disk. The enhanced Fe K line emission contains supplementary information to that of the persistent, radially integrated emission that is more often observed and measured. In theory, such hotspots may corotate with the accretion disk. The orbital timescale depends on the mass and spin of the central black hole and the distance from the black hole to the orbiting spot (e.g., Bardeen et al. 1972; Goosmann et al. 2006). In Figure 2 we show calculations of the orbital time versus distance from the innermost stable circular orbit for a black hole with a mass of $10^7\ M_\odot$ for five different values of a/M between 0 and 1. The orbital time can simply be scaled linearly for other masses. In the limit of large R, the curves converge to the simple Newtonian relation, $t_{orbit} \sim 100\pi\, R^{1.5}(M/10^7\ M_\odot)$ s, where R is in units of R_G.

A number of AGNs show observational evidence of emission from localized hotspots that originates in the inner regions of the accretion disk (e.g., Iwasawa et al. 1999; Turner et al. 2002; Guainazzi 2003; Iwasawa et al. 2004; Turner et al. 2006; Murphy et al. 2007). For example, during a flare seen in the *ASCA* data for MCG −6-30-15, the centroid of the Fe K line emission was observed to redshift from 6.4 keV to below 6 keV, implying that the profile was dominated by localized emission close to the black hole (Iwasawa et al. 1999). Similar behavior was found from the *RXTE* data of NGC 2992 (see Murphy et al. 2007). Theoretically, with long observations yielding high-resolution, high-throughput spectral data we will be able to detect full (possibly multiple) orbits of accretion-disk hotspots, depending on the black hole mass. In fact, Iwasawa et al. (2004) claim to have already observed four full, consecutive orbits of a hotspot around the black hole in NGC 3516 with *XMM-Newton*.

2.1. Method for Constraining Black Hole Spin

We develop the method that was suggested in Yaqoob (2001) for using the Fe K line resulting from a hotspot to constrain black hole spin. Properties of the Fe K line emission from hotspots have been discussed extensively in the literature (e.g., Nayakshin & Kazanas 2001; Goosmann et al. 2007; Dovčiak et al. 2008, and references therein). Here we formalize an approach to specifically use such emission to measure black hole spin. We emphasize that this work cannot yet be applied to current data since the available X-ray instrumentation does not have the required energy resolution and effective area.

In the remainder of this section we describe theoretical results pertaining to the Fe K line that make use of tables of transfer function[6] calculations that have been created for the nonaxisymmetric `kyr1line` model (Dovčiak et al. 2004). This model is included in a suite known as the "`KY` models" (Dovčiak et al. 2004) that are available for analyzing relativistic X-ray line profiles from black hole accretion disks in the Kerr metric. The routine `kyr1line` in particular models the instantaneous Fe K line profile function from the accretion disk for a given distance from the spin-dependent horizon radius ($R_d \equiv R - R_H$), inclination angle of the disk with respect to the observer (θ_{obs}), and azimuthal angle (ϕ) on the disk. We remind the reader that the model which we use here does not assume an axially symmetric accretion disk. Instead, localized spots can be tracked on the surface of the disk, taking all light-bending and time-delay effects into account.

[6] The usage of the term "transfer function" in the present paper (see Dovčiak et al. 2004 for a detailed description) does not include the time domain and should not be confused with the usage of the term in Yaqoob (2001) which does refer to the time domain.

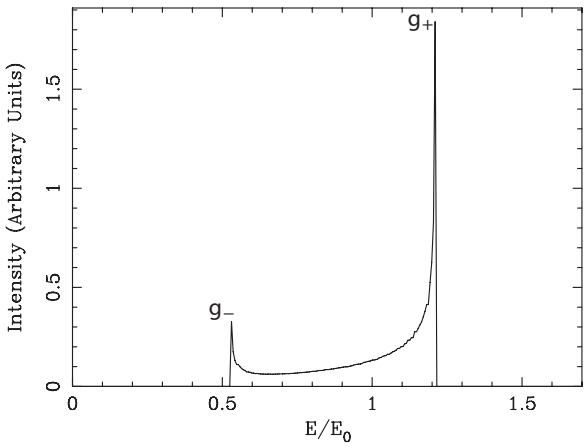

Figure 3. Example of an Fe K line profile function from the `kyr1line` model for $\theta_{\rm obs} = 60^\circ$ and $a/M = 0$, at a single radius of $R = R_{\rm MS} \equiv 6R_{\rm G}$ from the black hole. The x-axis is shown in units of energy-shift factor (g). In these units, the redshifted and blueshifted extrema may be defined as g_- and g_+, respectively.

Assuming that a hotspot completes at least one full orbit, tracing out an annulus around the disk, the resulting (temporally integrated) Fe K line emission will have a characteristic "double-horned" profile, with peaks corresponding to the extreme redshifts and blueshifts (due to Doppler and extreme gravitational effects) of the hotspot emission relative to the rest energy of the line. The more localized the hotspot is (that is, the narrower the annulus is), the sharper the two peaks of the profile will be.

In Figure 3 we show an example of a theoretical Fe K line profile function, which was produced with the `kyr1line` model. The emission in this example is calculated at a single radius of $R = 6R_{\rm G}$ from a black hole with $a/M = 0$, for a disk with an inclination angle of $\theta_{\rm obs} = 60^\circ$. We define the inclination angle with respect to the axis of the accretion disk, where $\theta_{\rm obs} = 0^\circ$ corresponds to a face-on observing angle and $\theta_{\rm obs} = 90^\circ$ corresponds to an edge-on observing angle. An inclination angle of 60° corresponds to the average of a distribution of randomly oriented disks. For inclination angles greater than 60°, disk-reflection features begin to diminish rapidly as the inclination angle increases (e.g., see George & Fabian 1991), and in AGNs, heavy line-of-sight obscuration may become problematic for inclination angles greater than 60°. The horizontal axis in Figure 3 is given in units of the energy-shift factor, $g \equiv E_{\rm obs}/E_0$, where $E_{\rm obs}$ is the observed energy at infinity and E_0 is the rest energy of the Fe K line from the emitting material. We refer to the g values of the red and blue extrema, for a given angular distribution of photon emission, as g_- and g_+, respectively. Figure 3 shows g_- and g_+ for isotropic emission in the disk frame, in which case g_- and g_+ correspond to the two peaks of the profile.

Given an angular distribution of photon emission from the orbiting hotspot co-rotating in the disk frame, the values of g_- and g_+ for the Fe K line profile of an orbiting hotspot depend only on the radial distance from the center of the black hole to the hotspot (R), the inclination angle of the accretion disk ($\theta_{\rm obs}$), and the black hole spin (a/M). In the present work we use transfer functions that assume isotropic emission in the disk frame. We therefore refer to g_- and g_+ synonymously with the g values of the peaks of the line profile. However, the `KY` model allows one to specify a more complicated profile of limb-darkening or limb-brightening (see Dovčiak et al. 2004). For the moment we neglect the effects of the finite size of the hotspot and calculate the best possible constraints before gradually introducing practical uncertainties.

It may be possible to obtain robust measurements of $\theta_{\rm obs}$ independently by modeling the time-averaged, radially integrated Fe K line profile (that is, the emission across the entire accretion disk). The inclination angle is mainly affected by the blue-wing cut-off of the Fe K line profile, and is not sensitive to the other disk parameters or black hole spin. This is because the maximum blueshift is due to the Doppler-shift maximum corresponding to emission from a particular radius of the disk. Emission from inside this particular radius is gravitationally redshifted away from the blue-wing cut-off, and outside this radius the Doppler blueshift decreases for a given $\theta_{\rm obs}$ because of the lower Keplerian velocities at larger radii. If the outer radius of emission is larger than the radius that produces the largest blueshift (as, from observation, generally appears to be the case), the blue wing is then mostly affected by $\theta_{\rm obs}$. Changes in the inner disk radius or in the steepness of the radial emissivity function mainly affect the red wing and not the blue cut-off because the entire Doppler profiles from the inner radii are gravitationally redshifted. Thus, if $\theta_{\rm obs}$ can be measured in this way, measurements of g_- and g_+ from a hotspot emission-line profile should then give constraints on the distance to the hotspot (R) and the black hole spin (a/M) since they are associated with two equations for two unknown quantities. This, of course, assumes that we know the ionization state of Fe, since g depends on the rest-frame energy of the emission line. We address this uncertainty in Section 2.2.

Values of g_- and g_+, for discrete values of R, $\theta_{\rm obs}$, and a/M, may be extracted from each of the line-profile functions that are stored in the `kyr1line` model tables. Once these values of g_- and g_+ have been compiled, they can then be interpolated (in each of the three variable directions) to construct curves of a/M versus R for a given inclination angle and any chosen constant value of g_- and g_+. Thus, one can construct a/M versus R contours for any measured pair of g_- and g_+ values when $\theta_{\rm obs}$ is already known. For a general (nonisotropic) angular distribution of emission, when the peaks of the line profile do not occur at g_- and g_+, the observed g values of the profile peaks may be calculated and related to a/M and R instead of g_- and g_+.

In Figure 4, we illustrate how this information can potentially determine constraints on a/M and R from a temporally integrated Fe K line profile from a complete orbit of a localized accretion-disk hotspot. In this example, we assume that $\theta_{\rm obs}$ has been independently measured to be 60° (from the persistent Fe K emission, which has been radially integrated across the *entire* emitting region of the accretion disk). We will deal with the effect of measurement uncertainties in $\theta_{\rm obs}$ in Section 2.2. Further suppose, for this example, that we measure red and blue peak energies from the emission of an orbiting hotspot to be $g_- = 0.22$ and $g_+ = 1.04$. Given these three variables (in practice, obtained from the data), we are then able to construct a/M versus R curves for the measured g_- and g_+ values. The units of distance to the hotspot are shown in Figure 4 as distance from the horizon radius ($R_{\rm d}$), as they are given in the transfer-function tables. The solution for the black hole spin and the distance to the hotspot is found at the intersection of the g_- and g_+ curves. Therefore, for the example shown in Figure 4, the distance to the hotspot (from the horizon) is $\sim$1.3 $R_{\rm G}$ and the spin is maximal ($a/M \sim 1$). We overlay the boundary corresponding to $R_{\rm MS}$ on Figure 4 (dashed line). The region above this line contains pairs of values (a/M, $R_{\rm d}$) that pertain to hotspot orbits only at

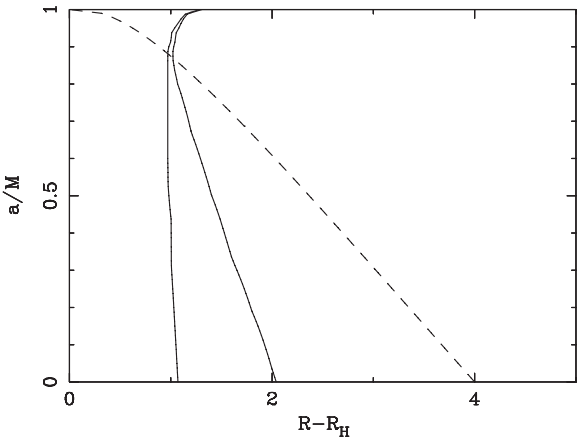

Figure 4. Curves of a/M vs. distance to the hotspot from $R_{\rm H}$, the horizon radius, ($R_{\rm d}$) for $g_- = 0.22$ (left-hand, solid curve) and $g_+ = 1.04$ (right-hand, solid curve), with $\theta_{\rm obs} = 60^\circ$. The dashed line represents the $R_{\rm MS}$ boundary. The solutions for the spin of the black hole and the distance to the hotspot are found at the intersection of the g_- and g_+ curves. Solutions that lie above the $R_{\rm MS}$ boundary curve correspond to orbits outside the ISCO ($R > R_{\rm MS}$).

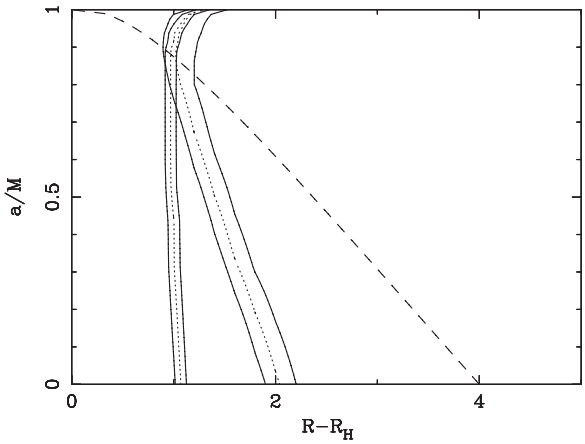

Figure 5. Curves of a/M vs. distance to the hotspot from the horizon radius ($R_{\rm d}$). The dotted curves are the same as those in Figure 4. These curves are overlaid with ±4.2% error boundaries for g_- (left-hand contour) and g_+ (right-hand contour), corresponding to the uncertainty in the ionization state of Fe.

radii larger than $R_{\rm MS}$ (see Section 3). For such hotspots with $R_{\rm d} < 4R_{\rm G}$, the $R_{\rm MS}$ boundary itself offers constraints on black hole spin. These constraints improve (in the sense of imposing a tighter range in a/M) as the orbital radius of the hotspot decreases.

2.2. Hotspot Fe K Line Measurement Uncertainties

The example shown in Figure 4 assumes the ideal case of a full orbit of a point-like hotspot, and does not include measurement uncertainties. When applied to real data, there are observational uncertainties that we must consider. With future high-resolution, high-throughput instruments, the largest uncertainty in the determination of g_- and g_+ (after the finite size of the hotspot) will be due to the unknown ionization state of Fe in the line emitting region. Note that the local ionization state in the vicinity of the hotspot may not necessarily be the same as the ionization state of the entire accretion disk. The rest energy of Fe K line emission must be some value between 6.404 keV (Fe I; see Bambynek et al. 1972) and 6.966 keV (Fe XXVI; see Pike et al. 1996). This corresponds to an uncertainty of ±4.2% in the measurement of g for the average rest-energy value in this range. We note, however, that the true error on g due to an incorrectly assumed value of the ionization state of Fe could be as large as twice this value. Shown in Figure 5 are the same g_- and g_+ curves as in Figure 4, overlaid with curves corresponding to this ±4.2% uncertainty. Given this uncertainty, the constraints on the black hole spin and the distance to the hotspot for the measured $\theta_{\rm obs}$, g_-, and g_+ are found in the overlap region of the two contours, shown in Figure 5.

To our knowledge, no method has yet been proposed for constraining the ionization state of Fe for a localized region of the accretion disk. If, in the future, it becomes possible to independently measure this ionization state (e.g., by using the Fe Kβ line in tandem with the Fe Kα line), then the largest uncertainty in actually measuring g_- and g_+ will be due to the absolute energy scale of the instrument. For future instruments, this could be as small as 1 eV, corresponding to an error of less than 0.02%, and we could therefore obtain much narrower g_- and g_+ contours. A separate source of error arises from uncertainties in the measurement of the disk inclination angle obtained from the radially integrated disk emission line. It can be expected that future instruments will yield $\theta_{\rm obs}$ measurements with uncertainties better than ±1°. Some current data already yield $\theta_{\rm obs}$ uncertainties of this order (e.g., Brenneman & Reynolds 2006). Figure 6, for example, shows the a/M versus $R-R_{\rm H}$ curves for $g_+ = 0.5$, for 29°, 30°, and 31°. We note that the error in $\theta_{\rm obs}$ produces a much less significant effect in the g_- and g_+ curves than that of the ionization uncertainty. However, the finite size of a hotspot will effectively give a finite width to the g_- and g_+ curves. If there is significant line emission away from the center of the hotspot, the effect on the width of the g_- and g_+ curves *could* be worse than that corresponding to the ionization uncertainty. The unknown angular distribution of photon emission from the hotspot could also yield greater uncertainty than that from the ionization state of Fe. For example, if the emission from the hotspot is highly anisotropic, the peak values measured from the data could correspond to values of g other than the g_- and g_+ values corresponding to the case of isotropic emission.

3. CONSTRAINING BLACK HOLE SPIN

It remains unclear whether the emission from within the ISCO contributes significantly to Fe K line emission from the accretion disk. Strictly speaking, a point-like hotspot could spiral past the ISCO, executing another orbit or more. In this case, radiation from the hotspot from within the ISCO could potentially contribute to the Fe K line profile, even if it is only a restricted transition region (e.g., see Reynolds & Fabian 2008). However, for a spirally infalling hotspot the g_- and/or g_+ peaks become distorted and broadened (e.g., see Hartnoll & Blackman 2002; Fukumura & Tsuruta 2004). In such cases, in practice, one would simply reject the data and search for another hotspot that had a cleaner signature. Thus, if we have a hotspot producing clearly defined g_- and/or g_+ peaks, the $R_{\rm MS}$ boundary gives a rough constraint on a/M and $R_{\rm d}$ for hotspots orbiting close to the black hole ($R_{\rm d} \equiv R - R_{\rm H} \leqslant 4$). In fact, this constraint is better than any constraint we could derive from the method described above, given the ±4.2% error from the uncertainty in the ionization state of Fe, as is clear in the example in Figure 5. We have also pointed out that additional uncertainties could result from the finite size of the hotspot and from the departure from isotropic emission in the disk frame. Furthermore, in the small $R_{\rm d}$ regime, measurement of just *one* peak (g_- *or* g_+) will

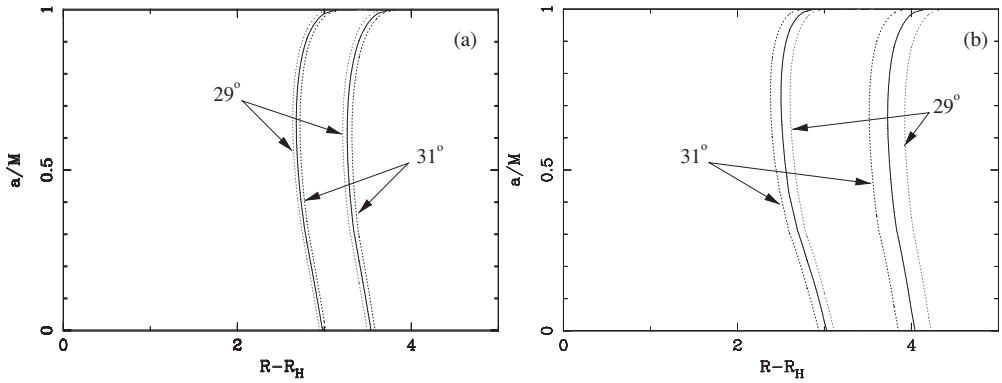

Figure 6. Uncertainty boundaries for ±4.2% for (a) $g_- = 0.519$ and (b) $g_+ = 0.892$, for $\theta_{obs} = 29°$(dotted), 30°(solid), and 31°(dotted). The effect of the ±4.2% uncertainty in the rest energy of the Fe K line due to the unknown ionization state is much greater than the ±1° uncertainty in θ_{obs} measurements.

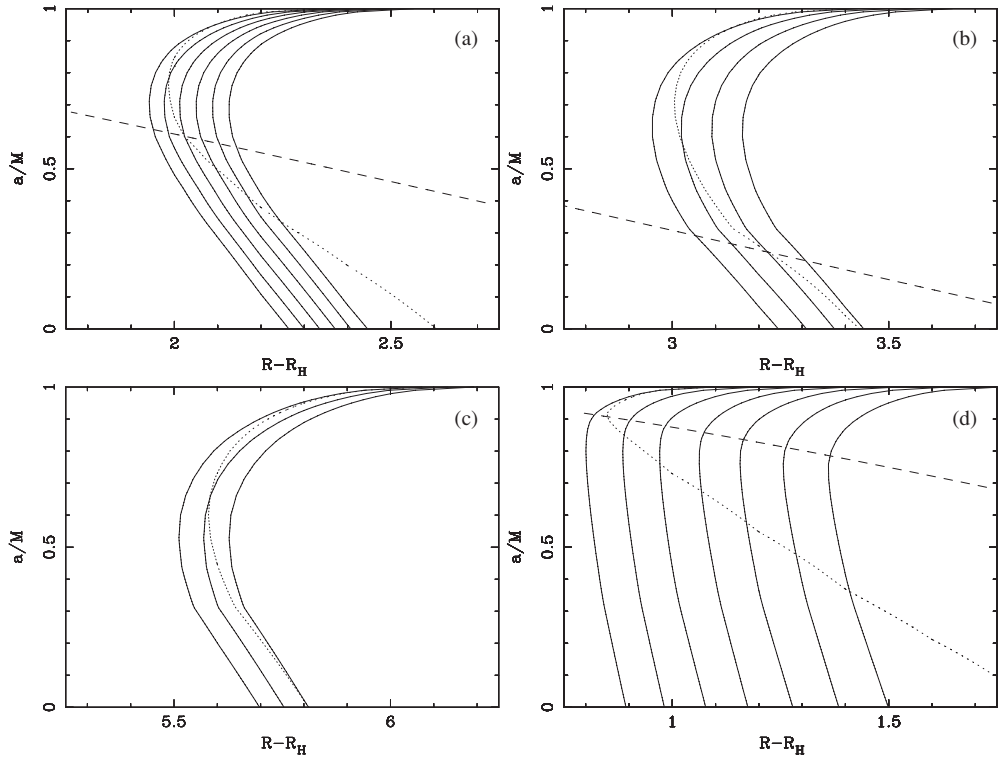

Figure 7. Curves of a/M vs. R_d for various values of g_- (solid) and g_+ ((a) 0.802, (b) 0.0892, and (c,d) 0.983; dotted), for $\theta_{obs} = 30°$ in panels (a)–(c), and 60° in panel d (see Section 3 for values of g_- and further details). Different pairs of (g_-,g_+) yield different solutions for the spin of the black hole and the distance to the orbiting hotspot. The overlaid, dashed line represents the R_{MS} boundary. Possible solutions occur at the intersection of the g_- and g_+ curves. Solutions above the R_{MS} boundary curve correspond to hotspot orbits that lie outside the ISCO ($R > R_{MS}$). In (c), all intersections are solutions that lie outside the ISCO.

yield such constraints from the R_{MS} boundary alone. Naturally, if the hotspot is orbiting at $R > 6R_G$ (corresponding to $R_d > 4R_G$ for $a/M = 0$ and $R_d > 5R_G$ for $a/M = 1$), the R_{MS} boundary does not constrain spin.

In Figure 7 we show examples of a/M versus R_d curves for possible measured values of g_+ (dotted), as well as curves for possible corresponding values of g_- (solid) for each g_+. Overlaid on each of these plots, where applicable, is the curve marking the boundary of R_{MS} (dashed line), as discussed in Section 2.1. In Figure 7(a), the dotted curve corresponds to a measurement of $g_+ = 0.802$, for $\theta_{obs} = 30°$; this is overlaid with (solid) curves corresponding to g_- values ranging from 0.426 to 0.446, with $\Delta g_- = 0.004$ (i.e., from left to right, g_- has values of 0.426, 0.430, 0.434, 0.438, 0.442, 0.446). These values clearly give distinct solutions for the value of a/M. Note that if we were only considering hotspots that complete full orbits outside of the ISCO ($R > R_{MS}$), then only the first three values of g_- would be acceptable solutions for the given g_+ value. In practice, the net effect of all the measurement uncertainties discussed in Section 2.2 must produce finite widths in the g_- and g_+ curves that are small enough to achieve the desired constraints on a/M. The Δg_- intervals shown in the examples in Figure 7 serve as a guide to what might be required (i.e., net uncertainties in g_- and g_+ better than $\sim 1\%$). Figures 7(b)–(d) show further examples of a/M versus R_d contour plots. In Figure 7(b), we show results for values of $g_+ = 0.892$ and $g_- = 0.519$ to 0.534 with $\Delta g_- = 0.005$ for $\theta_{obs} = 30°$. A plot for $g_+ = 0.983$, overlaid with $g_- = 0.649$, 0.651, and 0.653 for $\theta_{obs} = 30°$ is shown in Figure 7(c). This is an example of a hotspot orbiting in the regime where the R_{MS} boundary cannot constrain the spin. As θ_{obs} increases, g_- and g_+ are affected by larger Doppler shifts. In Figure 7(d) we show the

plot corresponding to the same g_+ value as in Figure 7(c) ($g_+ = 0.983$), but this time for a different inclination angle, $\theta_{\rm obs} = 60^\circ$. The solid curves correspond to $g_- = 0.190$ to 0.280, with $\Delta g_- = 0.015$.

We point out that the g_- and g_+ functions are more sensitive to the spin when the hotspot is closer to the black hole. We see in Figures 7(a)–(c) that, as the orbiting radius increases, the intersection of the g_- and g_+ contours becomes increasingly difficult to discern, making it more difficult to constrain a/M once measurement errors have been taken into account. However, the plots in Figure 7 also show that the technique described here has the *potential* to constrain the black hole spin using Fe K line profiles from orbiting hotspots, under favorable circumstances.

4. CONCLUSIONS

We have described a technique to measure black hole spin based on hotspots of enhanced Fe K line emission co-rotating in an accretion disk and studied the feasibility of the method. An advantage of the hotspot method is that it does not require knowledge of the Fe K line radial emissivity function over the disk. The method does not rely on measurement of line intensities, only peak energies (g_- and g_+) of narrow spectral features. However, achieving sufficiently small measurement uncertainties will be challenging and we have attempted to quantify the principal sources of uncertainty.

One caveat is that we assume that an independent measurement of the disk inclination angle, $\theta_{\rm obs}$, has been made from spectral fitting of the persistent, time-averaged, radially integrated Fe K emission. However, the measurement of $\theta_{\rm obs}$, which is most sensitive to the blue cut-off of the line emission, is much less dependent on the other parameters of the model than spin, although the derived $\theta_{\rm obs}$ is subject to some uncertainty due to the unknown ionization state of Fe. Another caveat is that departure from the assumptions of a standard, geometrically thin, optically thick, Keplerian disk may introduce additional uncertainties in the determination of black hole spin.

The technique described here *could*, in theory, be applied to real data obtained with future high-spectral-resolution and high-throughput X-ray instrumentation. In the present work we focused on the possibility of constraining spin from *one* Fe K emission line, most likely Fe Kα, due to a hotspot. We note that it may be possible to detect both Fe Kα *and* Fe Kβ emission, in which case we would have four separate contours to constrain a/M and $R_{\rm d}$ and we would furthermore be able to constrain the ionization state in the vicinity of the hotspot to lower than Fe XVII, as Fe Kβ cannot be produced for higher ionization states. Since the Fe Kα line energy for Fe XVII is 6.43 keV (e.g., Mendoza et al. 2004), the measurement uncertainties in g_- and g_+ could be as low as 0.5%. An additional possibility in the longer-term future is to measure the orbital radius using micro-arcsecond X-ray imaging instruments. This would facilitate remarkable constraints on black hole spin from hotspots.

It is also important to consider that these results assume observations of a *complete orbit* of a hotspot and, if it is unknown whether a full or partial orbit has been observed, there will be some ambiguity in the observed double-horned Fe K lines from hotspot observations. For this reason, this type of analysis would be best done with time-resolved spectroscopy, since the extreme redshift and blueshift could be more easily verified. Time-resolved spectroscopy of hotspots, under favorable conditions, may be possible with micro-calorimeters onboard planned missions. These instruments promise a spectral resolution of a few eV in the Fe K band combined with large effective area. Such X-ray spectroscopic instruments will not only be able to resolve these double-horned profiles, but will also yield *time-resolved* data that will allow us to break down the profile into multiple segments as the hotspot orbits the black hole. Therefore, with instrumentation on future missions, it may in principle be possible to "watch" an orbit with Fe K line profiles that incrementally redshift (and blueshift), tracing out the full, time-averaged, double-peaked profile. It would then be possible to constrain the orbital time of the hotspot. Given that $t_{\rm orbit}$ depends on M, a/M, and distance from the black hole to the hotspot, its measurement, in addition to the constraints on $R_{\rm d}$ obtained by the independent measurement of g_- and g_+ (as described here) may offer stronger constraints on the spin. This technique, however, could require more precise black hole mass measurements than those that are currently available. We defer an in-depth investigation of the feasibility of measuring spin with *time-resolved* X-ray spectroscopy to future work.

K.M. and T.Y. acknowledge partial support from NASA grant NNG04GB78A. V.K. and M.D. thank U.S.-Czech S&T cooperation project ME09036. K.M. and T.Y. thank J. H. Krolik, J. D. Schnittman, and S. C. Noble for discussions and comments.

REFERENCES

Bambynek, W., Crasemann, B., Fink, R. W., Freund, H.-U., Mark, H., Swift, C. D., Price, R. E., & Rao, P. V. 1972, Rev. Mod. Phys., 44, 716
Bardeen, J. M., Press, W. H., & Teukolsky, S. A. 1972, ApJ, 178, 347
Beckwith, K., Hawley, J. F., & Krolik, J. H. 2008, MNRAS, 390, 21
Blandford, R. D., & Znajek, R. L. 1977, MNRAS, 179, 433
Brenneman, L. W., & Reynolds, C. S. 2006, ApJ, 652, 1028
Czerny, B., Różańska, A., Dovčiak, M., Karas, V., & Dumont, A.-M. 2004, A&A, 420, 1
Dovčiak, M., Karas, V., Matt, G., & Goosmann, R. W. 2008, MNRAS, 384, 361
Dovčiak, M., Karas, V., & Yaqoob, T. 2004, ApJS, 153, 205
Fukumura, K., & Tsuruta, S. 2004, ApJ, 613, 700
Galeev, A. A., Rosner, R., & Vaiana, G. S. 1979, ApJ, 229, 318
Gammie, C. F., Shapiro, S. L., & McKinney, J. C. 2004, ApJ, 602, 312
George, I. M., & Fabian, A. C. 1991, MNRAS, 249, 352
Goosmann, R. W., Czerny, B., Mouchet, M., Karas, V., Dovčiak, M., Ponti, G., & Różańska, A. 2006, Astron. Nachr., 327, 977
Goosmann, R. W., Mouchet, M., Czerny, B., Doviak, M., Karas, V., Różańska, A., & Dumont, A.-M. 2007, A&A, 475, 155
Guainazzi, G. 2003, A&A, 401, 903
Hartnoll, S. A., & Blackman, E. G. 2002, MNRAS, 332, 1
Islam, J. N. 1985, Rotating Fluids in General Relativity (Cambridge: Cambridge Univ. Press)
Iwasawa, K., Fabian, A. C., Young, A. J., Inoue, H., & Matsumoto, C. 1999, MNRAS, 306, L19
Iwasawa, K., Miniutti, G., & Fabian, A. C. 2004, MNRAS, 355, 1073
King, A. R., Pringle, J. E., & Hofmann, J. A. 2008, MNRAS, 385, 1621
McClintock, J. E., & Remillard, R. A. 2006, in Cambridge Astrophys. Ser. 39, Compact Stellar X-ray Sources, ed. W. Lewin & M. van der Klis (Cambridge: Cambridge Univ. Press), 157
McClintock, J. E., Shafee, R., Narayan, R., Remillard, R. A., Davis, S. W., & Li, L.-X. 2006, ApJ, 652, 518
Mendoza, C., Kallman, T. R., Bautista, M. A., & Palmeri, P. 2004, A&A, 414, 377
Miller, J. M. 2007, ARA&A, 45, 441
Miller, J. M., Reynolds, C. S., Fabian, A. C., Miniutti, G., & Gallo, L. C. 2009, ApJ, 697, 900
Miller, J. M., et al. 2008, ApJ, 679, L113
Misner, C., Thorne, K., & Wheeler, J. 1973, Gravitation (San Francisco, CA: Freeman)
Murphy, K. D., Yaqoob, T., & Terashima, Y. 2007, ApJ, 666, 96
Nandra, K., O'Neill, P. M., George, I. M., & Reeves, J. N. 2007, MNRAS, 382, 194
Nayakshin, S., & Kazanas, D. 2001, ApJ, 553, L141
Peterson, B. M., & Benz, M. C. 2008, New Astron. Rev., 50, 797

Pike, C. D., et al. 1996, ApJ, 464, 487
Reynolds, C. S., & Fabian, A. C. 2008, ApJ, 675, 1048
Reis, R. C., Fabian, A. C., Ross, R. R., & Miller, J. M. 2009, MNRAS, 395, 1257
Shafee, R., McClintock, J. E., Narayan, R., Davis, S. W., Li, L.-X., & Remillard, R. A. 2006, ApJ, 636, 113
Thorne, K. S. 1974, ApJ, 191, 507
Turner, T. J., Miller, L., George, I. M., & Reeves, J. N. 2006, A&A, 445, 59
Turner, T. J., et al. 2002, ApJ, 574, 123
Yaqoob, T. 2001, in ASP Conf. Ser. 251, New Century of X-ray Astronomy, ed. H. Inoue & H. Kunieda (San Francisco, CA: ASP), 124
Yaqoob, T., & Padmanabhan, U. 2004, ApJ, 604, 63